8306-071

EFFECT OF COLD FORMING ON THE STRAIN-CONTROLLED FATIGUE PROPERTIES OF HSLA STEEL SHEETS

John M. Holt
United States Steel Corporation
Research Laboratory, Monroeville, PA

Philippe L. Charpentier
Wright State University
Dayton, Ohio
formerly with U.S. Steel Research

ABSTRACT

The effect of cold forming under different strain states on the strain-controlled fatigue properties of three hot-rolled sheet steels, ranging in thickness from 2.4 to 3.3 mm, was investigated. The steels were: a Dual Phase 80 steel (AISI 80DF), a 50-ksi minimum yield-strength HSLA steel (AISI 50XF), and, as a reference, a drawing-quality low-carbon aluminum-killed steel (AISI 1006). These steels were deformed to various strain levels (effective strains ranging from $\varepsilon_{eff} = 0.04$ to 0.6) using different modes of deformation to produce strain states similar to those found in formed parts: uniaxial tension, plane-strain deformation (cold rolling), and in-plane balanced biaxial stretching. Monotonic tension tests and strain-controlled fatigue tests were performed after deformation and also in the as-received, undeformed condition.

At long lives (longer than 10^4 to 10^5 reversals), the fatigue life was increased by prior deformation, whereas, at short lives, the fatigue life either remained the same or was reduced, depending on the mode of prior deformation and on the steel. The cyclic yield strength increased with the amount of prior deformation but less rapidly than the monotonic yield strength, reflecting the increased cyclic softening associated with the cold-worked microstructures.

HIGH-STRENGTH LOW-ALLOY (HSLA) hot-rolled sheet steels are used extensively to produce structural parts by cold forming. Since large amounts of deformation are often involved, the resulting mechanical properties can differ significantly from those of the as-received material. As a result, design procedures utilizing data measured on the as-hot-rolled material may not be suitable for predicting the fatigue-life performance of formed parts. Thus, it is necessary to know the fatigue properties of the material after forming.

The effect of prior deformation on the fatigue behavior of sheet steels has received some attention in recent years [1-6],* and is of continuing interest [7]. Fatigue properties have been determined after prestraining by simple tension [2-6], cold rolling [2,3,5], bending and unbending [4], and in-plane biaxial stretching [1]. In general, the effect of prior deformation on long-life behavior was found to be distinctly different from that on short-life behavior.

At <u>long lives</u> (generally greater than 10^4 to 10^5 reversals), for many of the steels investigated (yield strengths from 30 to 80 ksi), the fatigue life generally increased as a result of prior deformation [1-5]. However, a definite increase in fatigue life was not clearly observed in all cases [2-4,6]; for example, the fatigue life was shortened by prior deformation in some steels [2]; also, in most steels, the fatigue life appeared to be little affected when the amount of prior deformation was either small (<10% strain) [4,6] or very large (approximately 95% strain) [3]. The mode of prior deformation was reported to influence the fatigue life. For example, compressive prestrains produced by rolling were claimed to be less detrimental to the fatigue life than tensile prestrains produced by uniaxial tension [2].

At <u>short lives</u> (generally less than 10^4 to 10^5 reversals), in most steels and for most types of prior deformation investigated [1,2,4,5], the fatigue life (strain life) either decreased or remained the same as a result of prior deformation. However, in one instance [2] (a hot-rolled, low-carbon steel prestrained in tension), an increase in fatigue life with prior deformation was observed at very short lives,

---

* Numbers in brackets designate References at end of paper.

that is, at large total-strain amplitudes ($\Delta\epsilon_t/2 = 2\%$).

A large amount of cyclic softening, measured at an offset strain of 0.2 percent, has normally been observed after prior deformation regardless of the cyclic behavior in the undeformed condition [1,2,5,6]. In the undeformed condition, most steels cyclically softened [1,2,5], while some cyclically hardened [2] or remained cyclically stable [6]. After prestraining, cyclic hardening was observed in one instance [2].

The main purpose of this investigation was to document the influence of the amount of prior deformation (effective strain, ϵ_{eff}, up to 0.6) produced under various strain states typical of those encountered in sheet forming, Figure 1, on

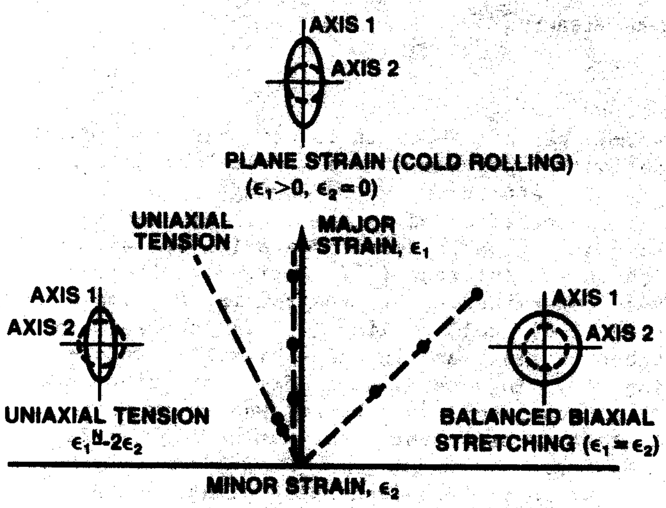

Fig. 1 - Three deformation modes investigated, as defined by surface strains, ϵ_1 and ϵ_2

the strain-controlled fatigue properties of three hot-rolled steels of different strength levels: two vanadium-bearing, rare-earth-treated, HSLA steels (AISI 50XF and AISI 80DF) and a reference, lower strength "drawing quality, special killed" steel, DQSK (AISI 1006). In addition, the effect of prior deformation on the monotonic tensile properties was also obtained.

For each steel, the following information was generated both for the undeformed condition and for each combination of deformation mode and amount of deformation: 1) strain-life curves (obtained from strain-controlled tests of smooth specimens), and 2) monotonic and cyclic stress-strain curves. All specimens were tested without machining the original mill surfaces ("as-received specimens").

EXPERIMENTAL METHODS

MATERIALS - Cut-to-length sheets of the three steels were obtained in the pickled and oiled condition. The chemical compositions are shown in Table 1. Sheets from single coils of 1006 and 50XF were tested, whereas sheets from two coils of 80DF were tested. The tensile properties in the as-received condition are shown in Table 2. Note that because of the difference in yielding behavior between 1006 and 50XF steels (discontinuous versus continuous yielding, respectively), the difference in yield strength between the two steels [approximately 70 MPa (10 ksi)] was less than the difference in tensile strength [approximately 105 MPa (15 ksi)]. To prevent strain aging in the 1006 steel, the sheets and test specimens were stored at 0°F throughout the program. The monotonic tensile properties of the two coils of 80DF were similar.

PREPARATION OF DEFORMED SAMPLES - The 50XF and 1006 steels were deformed to three levels of effective strain,* ϵ_{eff}, nominally 0.2, 0.4, and 0.6, in two deformation modes: in-plane balanced biaxial stretching (BBS), and cold rolling (CR). The 80DF steel was deformed in balanced biaxial stretching to $\epsilon_{eff} = 0.16$ and in uniaxial tension (UT) to $\epsilon_{eff} = 0.04$, 0.05, and 0.08. In all cases, large samples of the cut-to-length sheets were deformed, as described below, and then the test specimens were machined from these samples. The samples were electrochemically gridded with 2.5- or 5-mm-diameter circles before deformation to measure the principal surface strains, ϵ_1 and ϵ_2, from which ϵ_{eff} was then calculated.

In-plane balanced biaxial stretching was produced by the technique first proposed by Marciniak, et al. [8]: a cylindrical flat-bottom punch is used, and an auxiliary blank containing a central circular hole is placed between the punch and the sheet to be stretched. Perfectly flat, 76-mm-diameter (3 inch) samples essentially free from strain gradients were produced with strains up to $\epsilon_{eff} \approx 0.6$ in near-balanced biaxial stretching ($1 < \epsilon_1/\epsilon_2 < 1.17$ for the various samples produced).

Cold rolling parallel to the hot-rolling direction was produced in 200-mm-wide (8 inch) samples of AISI 50XF and 1006 using a laboratory mill with 216-mm-diameter (8.5 inch) work rolls. The bulk of the 50XF steel was rolled to effective strains of 0.2, 0.3, and 0.57, but the monotonic tension specimens were taken from material rolled to $\epsilon_{eff} = 0.2$, 0.38, and 0.57. The 1006 steel was rolled to effective strains of 0.19, 0.38, and 0.61.

Uniaxial tension in the 80DF steel was produced in large samples, 300- to 380-mm (12 to 15 inches) wide by 1200-mm (48 inches) long, that

---

* The isotropic effective strain, ϵ_{eff}, which, in the case of proportional straining, can be defined by:

$$\epsilon_{eff} = \sqrt{2}/3 \left[(\epsilon_1 - \epsilon_2)^2 + (\epsilon_2 - \epsilon_3)^2 + (\epsilon_3 - \epsilon_1)^2\right]^{1/2} \tag{1}$$

is used here as a common measure of the overall amount of deformation in comparing the various strain states. ϵ_1, ϵ_2, and ϵ_3 are the principal strains.

Table 1 - Chemical Compositions of the Three Steels (in Weight Percent)

Steel	C	Mn	Si	S	P	N	Al (Total)	Cb	V	Ce
AISI 1006	0.057	0.25	0.005	0.015	0.007	0.005	0.039	<0.005	<0.002	<0.001
AISI 50XF	0.11	0.68	0.48	0.014	0.004	0.007	0.055	<0.005	0.017	0.015
AISI 80DF(1)										
Sheet 1	0.12	1.55	0.64	0.010	0.009	0.007	0.062	-	0.046	0.017
Sheet 2	0.12	1.72	0.57	0.012	0.006	0.007	0.063	-	0.043	0.017

(1) Sheet 1, 18.7% martensite; sheet 2, 17.7% martensite

Table 2 - As-Received Tensile Properties (2-Inch Gage Length Specimens)(1)

Steel	Thickness, mm	Specimen Orientation	Yield Strength, MPa	Tensile Strength, MPa	Yield Point Elongation, %	Uniform Elongation, %	Total Elongation in 2 Inches, %
AISI 1006	3.0	Longitudinal	278(2)	367	0.95	20.8	38.5
		Transverse	295	365	1.6	18.1	33.5
AISI 50XF	3.1	Longitudinal	366	469	0.0	19.5	31.5
		Transverse	347	462	0.0	19.4	32.0
AISI 80DF							
Sheet 1	2.4	Longitudinal	403	667	0.0	19.3	33.5
Sheet 2	3.3	Longitudinal	408	664	0.0	17.2	30.5
		Transverse	431	652	0.0	16.2	30.0

(1) Each reported value is the average of two or three tests.
(2) A very small upper yield point was observed in these specimens.

Conversion Factors:
1 ksi = 6.89 MPa
1 inch = 25.4 mm

were stretched parallel to the hot-rolling direction in a large-capacity tensile machine.

Figure 2 shows the orientations of the test specimens with respect to the hot-rolling direction (HRD) and to the axes of the cold deformation for the three modes of deformation. In the case of uniaxial tension (80DF steel), tests were conducted both parallel and perpendicular to the direction of prior tension to investigate anisotropy effects.

The tensile and fatigue properties after CR and after BBS were measured in the HRD, that is, parallel to the prior tensile strain. Transverse properties were not measured after these two modes of deformation because previous work had shown 1) that the fatigue life exhibited essentially no anisotropy in various HSLA sheet steels containing different types of inclusions [4,6,9]* and 2) CR and BBS, in low-carbon and HSLA steels, produced only a small deformation-induced yield-strength anisotropy or none at all [10]. Because

* Steels with 50-ksi minimum yield strength containing either manganese silicates and manganese sulfides or alumina and zirconium sulfides [4], 80DF steel containing alumina and rare-earth sulfides [6], and 50-ksi minimum yield-strength steel (50XF) containing alumina and rare-earth sulfide inclusions [9].

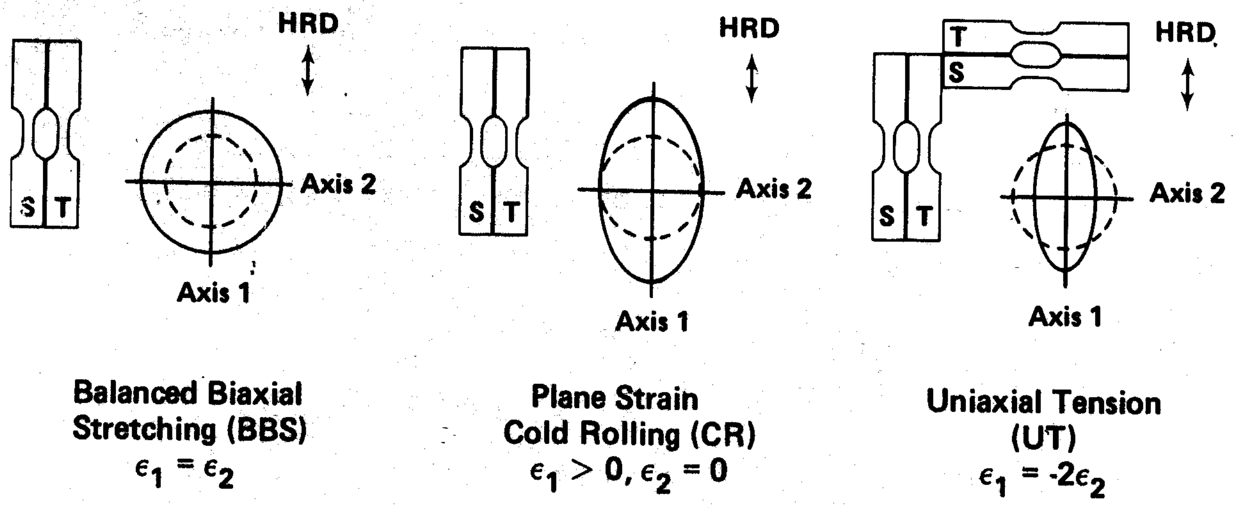

Fig. 2 - Modes of deformation and specimen orientations investigated. ↕ HRD indicates the hot rolling direction, S and T signify strain-controlled fatigue-test specimens and tension-test specimens, respectively

a yield-strength anisotropy was previously observed after UT, the tensile and fatigue properties were measured both parallel and perpendicular to the HRD.

MONOTONIC TENSION TESTS AND FATIGUE TESTS - The monotonic 0.2 percent offset yield strength (0.2MYS), tensile strength (TS), uniform elongation, and total elongation, were measured in the undeformed condition parallel to the hot-rolling direction and also for each mode of deformation and specimen orientation as a function of ε_{eff}, using the specimen shown in Figure 3.

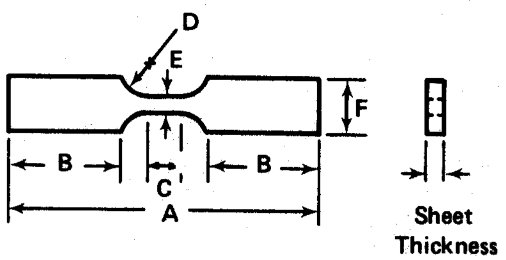

Dimensions, mm					
A	B	C	D	E	F
50 to 75	Approx. 12 to 25	8.64	9.40	4.57	12.7

1 inch = 25.4 mm

Fig. 3 - Specimen used for tension and fatigue tests

Strain-controlled fatigue tests were conducted with the same specimen in accordance with ASTM practice E606-80 [11] to obtain the strain-life curve corresponding to each combination of deformation mode, prior strain level, and specimen orientation (Table 3). The tests were performed under constant-amplitude, completely reversed, strain-controlled, axial-load using hydraulic, closed-loop, testing machines and Wood's metal grips. Total strain, measured by an extensometer with a 7.6-mm (0.300 inch) gage length, was the control parameter. For each combination in Table 3, tests were generally conducted on duplicate specimens at the following nominal total-strain amplitudes: 0.75×10^{-2}, 0.5×10^{-2}, 0.25×10^{-2}, and 0.15×10^{-2}, or 0.125×10^{-2}. The extensometer was mounted with the knife edges against the machined sides of the specimen, not against the sheet surface. The strain-time wave form was sinusoidal with the first half cycle positive. To minimize the strain-rate variation between the tests conducted at the different strain amplitudes, the sinusoidal frequency was increased from 0.2 to 3 Hz as the nominal strain amplitude was decreased, resulting in average strain rates ranging from 0.6 to 1.5 sec^{-1}. For each specimen, the stress-strain response was recorded during the initial loading and during the first few strain cycles. Then, hysteresis loops were recorded periodically throughout the test to monitor the cyclic response to obtain the half-life values of the various cyclic parameters described later. The tests were terminated either when a fatigue crack corresponding to a drop in load of about 20 to 30 percent was detected (presence of a cusp in the hysteresis loop) or after 2-million reversals (runout specimens).

For each specimen, from the hysteresis loop nearest half-life, the total-strain range, $\Delta\varepsilon_t$, was partitioned into its elastic and plastic components, $\Delta\varepsilon_e$ and $\Delta\varepsilon_p$ as shown in Figure 4 [13]. The modulus of elasticity, E, and the stress range, $\Delta\sigma$, were also obtained from the same hysteresis loop.

The strain-life behavior was examined by plotting the total-strain amplitude, $\Delta\varepsilon_t/2$, versus $\log(2N_f)$,* the number of reversals to failure

* $\Delta\varepsilon_t/2$, rather than the more commonly used $\log(\Delta\varepsilon_t/2)$, was plotted to better show small differences in behavior.

Table 3 - Testing Program Summary

Nominal Effective Strain Level	All Steels: Undeformed, As-Received Surfaces (1)	AISI 1006 and AISI 50XF Steel: Cold Rolling (CR) (1)	AISI 1006 and AISI 50XF Steel: In-Plane Balanced Biaxial Stretching (BBS) (1)	AISI 80DF Steel: Uniaxial Tension (UT)	AISI 80DF Steel: In-Plane Balanced Biaxial Stretching (BBS) (1)
0.0	T,S	-	-	-	-
0.04 to 0.08	-	-	-	T,S	-
0.2	-	T,S	T,S	-	T,S
0.4	-	T,S	T,S	-	-
0.6	-	T,S	T,S	-	-

(1) All the test specimens were oriented parallel to the HRD except in AISI 80DF in the undeformed condition and after uniaxial tension, in which cases they were oriented parallel and perpendicular to the HRD, i.e., parallel and perpendicular to the direction of prior tension (see Figure 2).

T: Tension tests.
S: Strain-controlled fatigue tests.

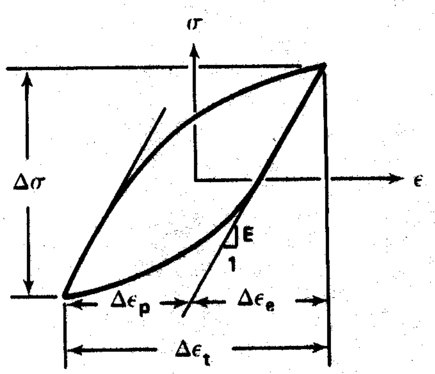

Fig. 4 - Stress-strain hysteresis diagram

for each condition shown in Table 3 and these strain-life plots were compared visually to assess the effect of prior deformation. Also, regression equations relating the elastic and plastic strain amplitude, $\Delta\varepsilon_e/2$ and $\Delta\varepsilon_p/2$, to $2N_f$, were obtained by fitting straight lines* to the data pairs log $(\Delta\varepsilon_e/2)$, log $(2N_f)$ and log $(\Delta\varepsilon_p/2)$, log $(2N_f)$ using the least-square method. The regression equations are:

$$\log \frac{\Delta\varepsilon_e}{2} = b \log (2N_f) + \log\left(\frac{\sigma_f'}{E}\right) \qquad (2)$$

$$\log \frac{\Delta\varepsilon_p}{2} = c \log (2N_f) + \log (\varepsilon_f') \qquad (3)$$

The strain-life fatigue constants b, σ_f', c, and ε_f' where b = fatigue strength exponent, σ_f' = fatigue strength coefficient, c = fatigue ductility exponent, and ε_f' = fatigue ductility coefficient were thus obtained both in the deformed and undeformed conditions. Combining Eq. (2) and (3), the total strain amplitude, $\Delta\varepsilon_t/2 = \Delta\varepsilon_e/2 + \Delta\varepsilon_p/2$, is given by:

$$\frac{\Delta\varepsilon_t}{2} = \frac{\sigma_f'}{E} (2N_f)^b + \varepsilon_f' (2N_f)^c. \qquad (4)$$

Cyclic stress-strain curves for each condition in Table 3 were constructed using the relationship:

$$\frac{\Delta\varepsilon_t}{2} = \frac{\Delta\sigma}{2E} + \left(\frac{\Delta\sigma}{2K'}\right)^{1/n'} \qquad (5)$$

where K', the cyclic strength coefficient, and n', the cyclic strain-hardening exponent, are determined from linear-regression fits of the data pairs $\Delta\sigma/2$ and $\Delta\varepsilon_p/2$ according to the relationship:

$$\log \frac{\Delta\sigma}{2} = n' \log \left(\frac{\Delta\varepsilon_p}{2}\right) + \log K'. \qquad (6)$$

Each cyclic stress-strain curve was then compared to the corresponding monotonic stress-strain curve to assess the effect of cyclic

* Previous work [6] had shown that for undeformed steel, the fit of strain-life data by a straight line was as good as by a sixth-order polynominal.

deformation on stress-strain behavior for the various modes and amounts of deformation. Each monotonic stress-strain curve used for the comparison was the average of the initial loading curves for the specimens cyclically tested at nominal $\Delta\varepsilon_t/2 \geq 0.5 \times 10^{-2}$ (generally a total of four specimens).

RESULTS - POSTFORMED TENSILE PROPERTIES

The monotonic yield strength, tensile strength, uniform elongation, and total elongation for the three steels after the various modes and amounts of deformation are shown in Table 4 and briefly discussed below.

Table 4 - As-Received and Postformed Monotonic Tensile Properties of the Three Steels (0.3-Inch Gage Length Specimen)

Mode of Deformation	Specimen Orientation	Nominal Effective Strain	0.2% Offset Yield Strength, MPa	Tensile Strength, MPa	Uniform Elongation, %	Total Elongation in 0.3 Inch, %
			DQSK AISI 1006			
Undeformed	Longitudinal	0.0	282	350	21.2	56.4
Balanced Biaxial Stretching	Longitudinal	0.2	475	502	1.2	27.4
		0.4	557	564	0.9	20.4
		0.6	579	583	0.7	16.0
Cold Rolling	Longitudinal	0.19	495	514	0.4	27.8
		0.38	534	562	0.8	21.7
		0.61	586	617	0.6	15.8
			AISI 50XF			
Undeformed	Longitudinal	0.0	349	471	23.1	52.9
Balanced Biaxial Stretching	Longitudinal	0.2	579	606	1.4	27.8
		0.4	644	675	1.8	19.6
		0.6	661	713	1.7	15.4
Cold Rolling	Longitudinal	0.20	553	564	1.6	29.2
		0.30	575	628	1.7	24.0
		0.57	673	696	1.1	16.6
			AISI 80DF(1)			
Undeformed	Longitudinal(2)	0.0	406	666	18.2	32.0
	Transverse		431	652	16.2	30.0
Balanced Biaxial Stretching	Longitudinal	0.16	726	813	2.0	11.5
Uniaxial Tension	Longitudinal	0.04	579	683	10.2	23.0
	Longitudinal	0.05	624	690	7.3	26.5
	Longitudinal	0.08	659	697	5.6	23.0
	Transverse	0.08	515	691	6.7	18.5

(1) 2.00-inch gage length specimens
(2) Average of both sheets (Table 2)

Conversion Factor:
1 ksi = 6.89 MPa

AISI 1006 STEEL - Both the yield strength and the tensile strength are essentially the same for the two modes of deformation and they both increase rapidly with the amount of deformation, Figure 5. The strain hardening capacity decreases rapidly initially, as evidenced by the rapid increase in the yield-to-tensile ratio, Figure 5. The uniform elongation also decreased rapidly between $\varepsilon_{eff} = 0$ and $\varepsilon_{eff} = 0.2$; the total elongation decreases more gradually with prior strain, Table 4.

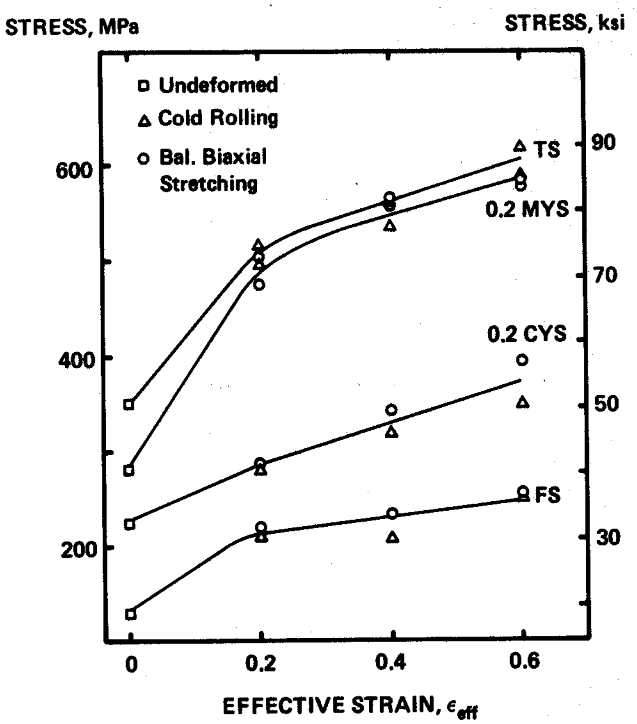

Fig. 5 - AISI 1006 steel—mechanical properties after deformation as a function of prior effective strain

AISI 50XF STEEL - The effect of prior deformation on the postformed tensile properties was generally similar to that observed for 1006 steel, Figure 6 and Table 4. Interestingly, the postformed uniform elongation was slightly larger in 50XF than in 1006 steel; the postformed total-elongation values for the two steels were nearly identical, Table 4.

AISI 80DF STEEL - The postformed yield strength in the direction of prior tension, after uniaxial tension, appeared to be the same as after BBS, Figure 7. In the direction normal to the prior tension, the yield strength was much lower, a Bauschinger-type effect. In contrast to the yield strength, the tensile strength exhibited no anisotropy after uniaxial tension, i.e., the yield strength was the same parallel and perpendicular to the prior tension. Interestingly, the tensile strength appeared to be much higher after BBS than after UT, even though the yield strength was the same, suggesting a dependence of

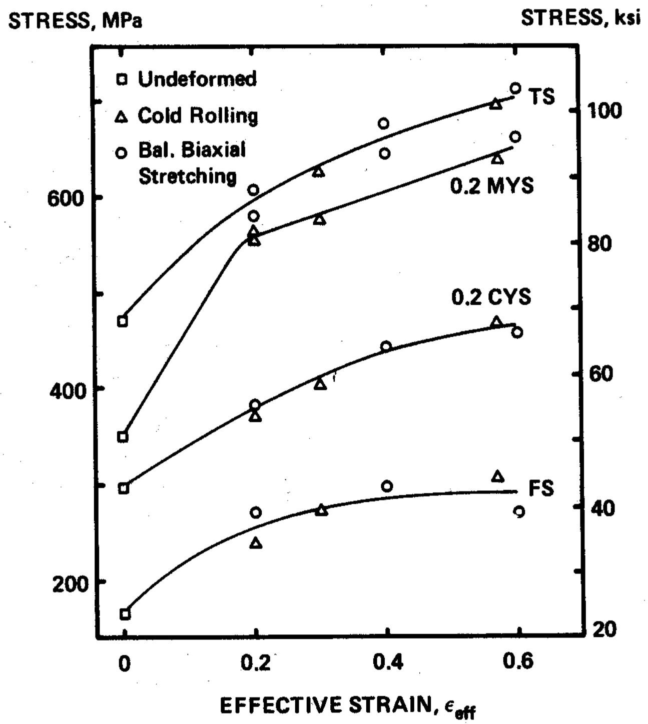

Fig. 6 - AISI 50XF steel—mechanical properties after deformation as a function of prior effective strain

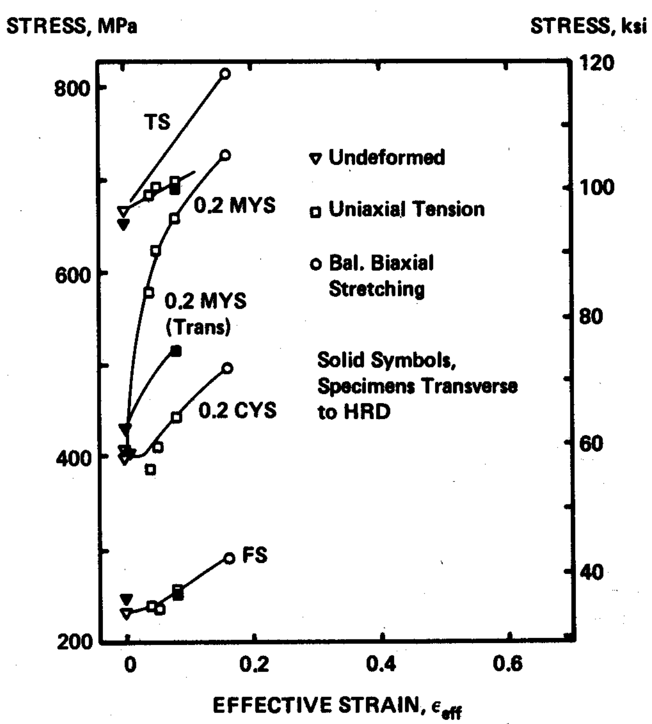

Fig. 7 - AISI 80DF steel—mechanical properties after deformation as a function of prior effective strain

the residual strain hardening capacity on the mode of prior deformation.

RESULTS - STRAIN-LIFE BEHAVIOR

The effect of mode and amount of deformation on the strain-life behavior of each steel was assessed by comparing the strain-life plots before and after deformation. For clarity, individual data are not shown for the undeformed material but bands including all the data points were drawn. The constants for Eq. (4) are listed in Table 5 for the three steels for each deformation mode and effective-strain level investigated. These constants were used to calculate the total strain amplitude at a life of 2×10^6 reversals for the various modes and amounts of deformation. From these values of total strain

Table 5 - Strain-Life Fatigue Constants and Fatigue Strength After the Various Modes of Prior Deformation

			Strain Life Fatigue Constants				Fatigue Strength at 2×10^6 Reversals, FS	
			Plastic-Strain vs Reversals		Elastic-Strain vs Reversals			
Mode of Deformation	Specimen Orientation	Nominal Effective Strain	Slope, c (Fatigue Ductility Exponent)	Intercept, ε_f' (Fatigue Ductility Coefficient)	Slope, b (Fatigue Strength Exponent)	Intercept, (σ_f'/E), $\times 10^{-3}$	Total-Strain Amplitude $\times 10^{-3}$	Stress, MPa
				AISI 1006 Steel				
Undeformed	Longitudinal	0.0	-0.4543	0.1564	-0.1172	3.5483	0.86	131
Balanced Biaxial Stretching	Longitudinal	0.2	-0.6314	0.6029	-0.0680	2.8352	1.12	220
		0.4	-0.7095	0.9527	-0.0777	3.4433	1.15	234
		0.6	-0.8932	2.7123	-0.0737	3.6071	1.24	255
Cold Rolling	Longitudinal	0.19	-0.5183	0.2354	-0.0701	2.9063	1.18	208
		0.38	-0.6557	0.5902	-0.0816	3.5334	1.13	207
		0.61	-0.5571	0.2301	-0.0879	4.2062	1.25	251
				AISI 50XF Steel				
Undeformed	Longitudinal	0.0	-0.5676	0.4239	-0.1181	4.3622	0.90	165
Balanced Biaxial Stretching	Longitudinal	0.2	-0.7152	1.1384	-0.0758	3.9551	1.35	269
		0.4	-0.5353	0.1007	-0.0729	4.1180	1.47	296
		0.6	-0.6582	0.3267	-0.1018	5.6741	1.32	269
Cold Rolling	Longitudinal	0.20	-0.6388	0.7000	-0.0921	4.3220	1.20	238
		0.30	-0.5367	0.2136	-0.0835	4.2114	1.34	272
		0.57	-0.5314	0.1651	-0.0842	5.1189	1.58	307
				AISI 80DF Steel				
Undeformed	Longitudinal	0.0	-0.6880	0.9783	-0.1096	5.568	1.18	234
	Transverse	0.0	-0.6978	0.9480	-0.0973	5.050	1.27	248
Balanced Biaxial Stretching	Longitudinal	0.16	-0.8241	2.4168	-0.1089	6.835	1.42	291
Uniaxial Tension	Longitudinal	0.04	-0.6988	1.0523	-0.1067	5.333	1.18	240
	Longitudinal	0.05	-0.6812	0.9021	-0.1221	6.530	1.16	239
	Longitudinal	0.08	-0.6836	0.9997	-0.1056	5.886	1.32	258
	Transverse	0.08	-0.8636	3.5740	-0.1011	5.596	1.30	255

Conversion Factor:
1 ksi = 6.89 MPa

amplitude, the corresponding stresses were obtained using Eq. (5) (cyclic stress-strain curves). These stress values, which are the fatigue strength at 2 x 10^6 reversals, FS, are shown in Table 5 and plotted in Figures 5 to 7.

AISI 1006 STEEL - The strain-life plots for the two modes of deformation are shown in Figures 8a and 8b along with the data band for the

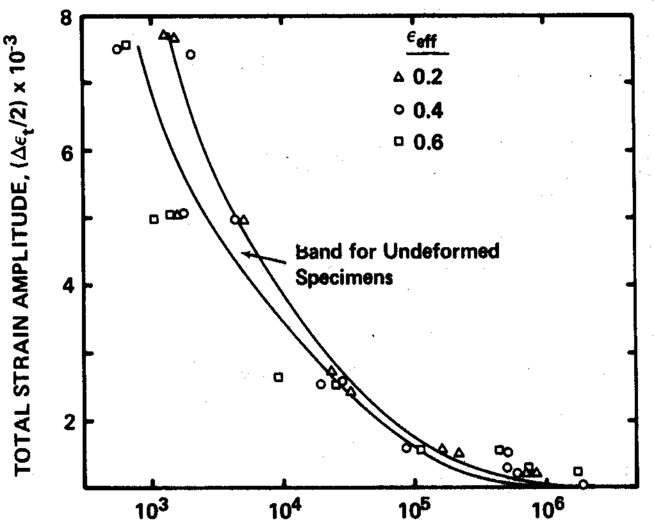

Fig. 8a - After balanced biaxial stretching

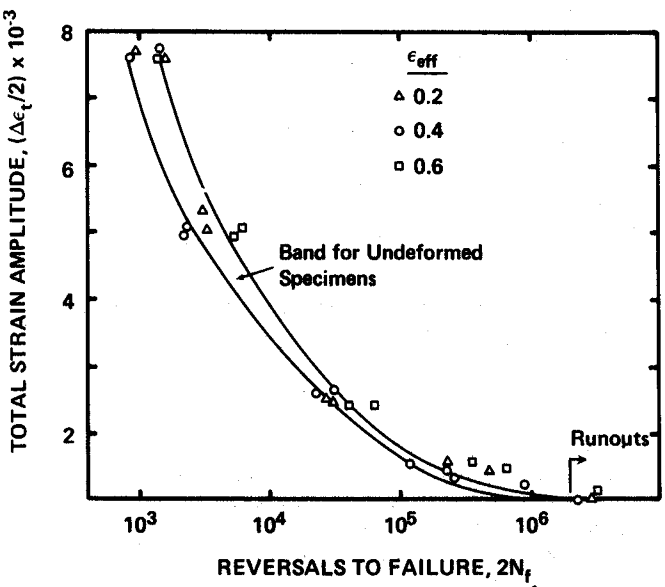

Fig. 8b - After cold rolling

Fig. 8 - AISI 1006 steel–strain-life curves after deformation

undeformed material. The effect of balanced biaxial stretching on fatigue life was as follows: at large strain amplitudes ($\Delta\epsilon_t/2 > \sim 2.5 \times 10^{-3}$), the fatigue life remained approximately the same or decreased slightly when compared to that of the undeformed material; in contrast, at small strain amplitudes the fatigue life increased as a result of the prior deformation. However, no clear correlation was observed between the fatigue life and the level of ϵ_{eff}, Table 5.

After cold rolling, the fatigue life was approximately the same as in the undeformed material at large strain amplitudes (short lives) but it was longer at small strain amplitudes (long lives). Thus, unlike BBS, CR appeared to cause no reduction in fatigue life at short lives. Another difference between the two deformation modes was that the scatter of the data was larger after BBS than after CR. Thus, BBS was somewhat more detrimental to the fatigue life than CR.

The fatigue-strength values at 2 x 10^6 reversals, determined using the fatigue-life constants and the cyclic stress-strain curves, are shown in Table 5 and plotted in Figure 5. The fatigue strength generally increased with the amount of deformation.

AISI 50XF STEEL - Although the effects of prior deformation by BBS or CR on the strain-life behavior of 50XF, Figure 9, were generally similar to those in 1006, some specific differences were apparent: 1) the effect of prior deformation was stronger for 50XF than for 1006 in that both the decrease in life at large strain amplitudes and the increase in life at small strain amplitudes were greater in 50XF than in 1006; and 2) the strain amplitude below which the fatigue life was increased by prior deformation appeared to be somewhat larger in 50XF than in 1006 (compare Figure 9 to Figure 8).

AISI 80DF STEEL - In this steel, the fatigue life appeared to remain unchanged or to increase very slightly as a result of deformation, at least for the effective strain levels investigated, Figure 10. Also, the fatigue life appeared to be unaffected by the mode of deformation and the specimen orientation. The strain-life fatigue constants before and after deformation are shown in Table 5. No statistically significant differences were found between these constants [6,19].

The fatigue limit of the BBS specimens is significantly lower than what would be expected based upon the tensile strength, an indication that BBS may be more damaging than UT.

RESULTS - CYCLIC STRESS-STRAIN BEHAVIOR

AISI 1006 STEEL - The cyclic stress-strain curves for 1006 for the various modes and amounts of deformation are shown in Figures 11a and 11b. These curves were constructed by evaluating Eq. (5) using the values of K′ and n′ shown in Table 6. Also shown in these figures for comparison are the corresponding monotonic stress-strain curves. As can be seen, both the cyclic and the monotonic 0.2 percent offset yield strengths (0.2CYS and 0.2MYS, respectively) increased as the amount of prior strain increased. Further, it can be seen that cyclic softening occurred for all conditions, including the undeformed material. These results are also

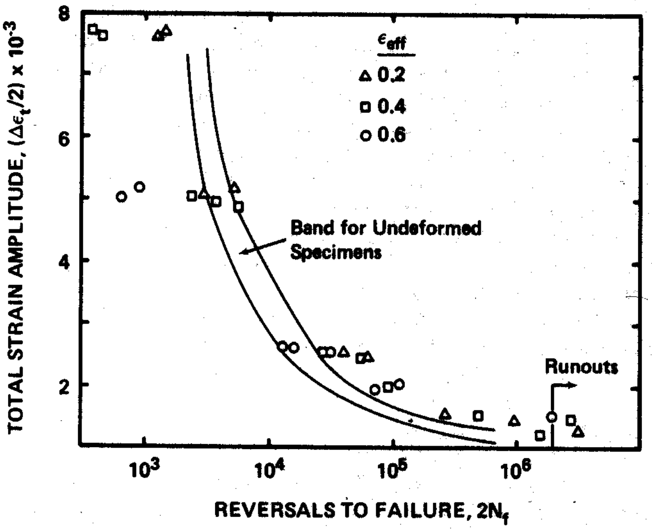

Fig. 9a. After Balanced Biaxial Stretching

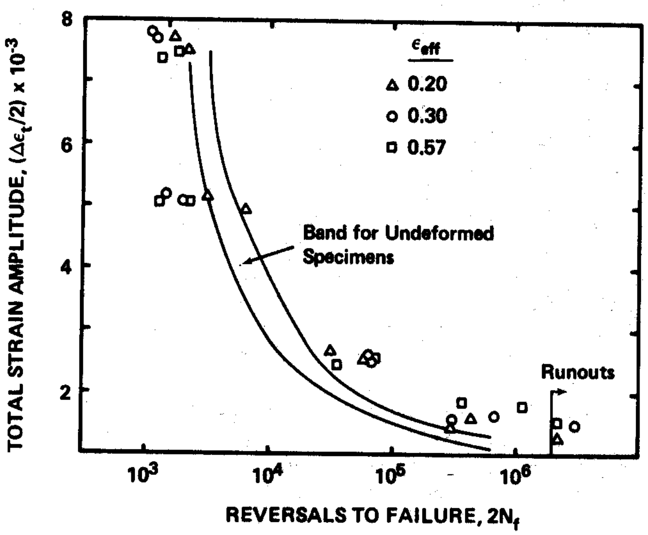

Fig. 9b. After Cold Rolling

Fig. 9 - AISI 50XF steel-strain-life curves after deformation

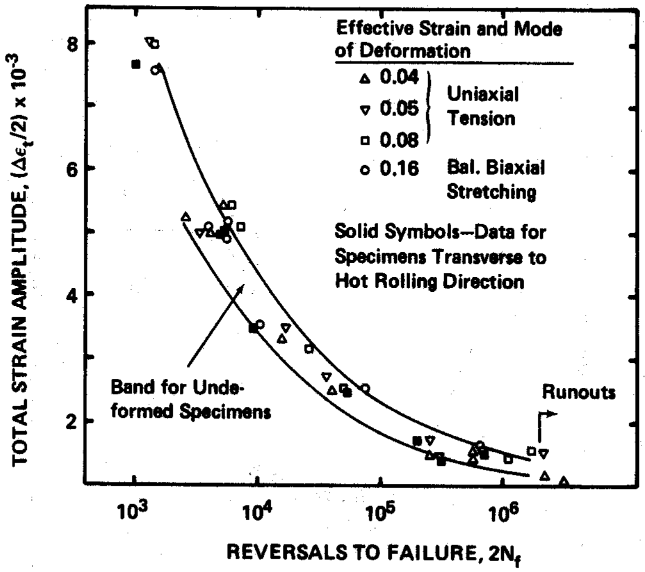

Fig. 10 - AISI 80DF steel-strain-life curves after deformation

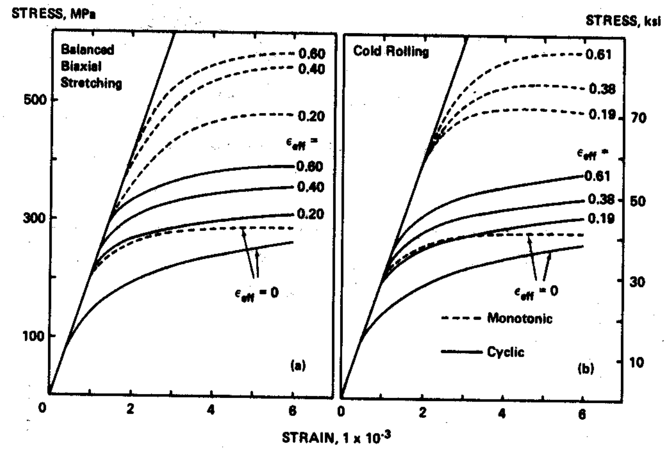

Fig. 11 - AISI 1006 steel-monotonic and cyclic stress-strain curves before and after deformation

shown in Figure 5 in which the 0.2CYS and the 0.2MYS are seen to be essentially independent of deformation mode and to increase approximately 21 and 28 MPa (3 and 4 ksi), respectively, per 0.1 increase in effective strain beyond ε_{eff} = 0.2. Figure 5 also shows that the amount of cyclic softening is far greater in the deformed condition than in the undeformed.

The degree of softening can also be seen in Table 6 which shows the 0.2CYS and 0.2MYS values as well as their ratios. The ratio between the cyclic and monotonic yield strengths for the deformed material is approximately the same regardless of the mode and amount of deformation (0.2CYS/0.2MYS ≈ 0.61) and it is smaller than for the undeformed material, (0.2CYS/0.2MYS = 0.8).

As seen in Table 6, a large decrease in both the cyclic strain hardening exponent, n′, and the

Table 6 - Comparison Between Cyclic Yield Strength and Monotonic Yield Strengths

Mode of Deformation	Specimen Orientation	Nominal Effective Strain	Cyclic Stress-Strain Constants: K', MPa (Cyclic Strength Coefficient)	Cyclic Stress-Strain Constants: n' (Cyclic Strain Hardening Exponent)	Cyclic Yield Strength, 0.2% Offset (0.2CYS), MPa	Monotonic Yield Strength, 0.2% Offset, (0.2MYS), MPa	0.2CYS/0.2MYS
AISI 1006							
Undeformed	Longitudinal	0.0	925.2	0.232	226	282	0.80
Balanced Biaxial Stretching	Longitudinal	0.2	468.7	0.077	288	475	0.61
		0.4	573.1	0.086	342	557	0.61
		0.6	555.1	0.064	393	579	0.68
Cold Rolling	Longitudinal	0.19	566.3	0.111	282	495	0.57
		0.38	575.9	0.095	318	534	0.60
		0.61	641.9	0.094	348	586	0.59
AISI 50XF							
Undeformed	Longitudinal	0.0	817.8	0.167	296	349	0.85
Balanced Biaxial Stretching	Longitudinal	0.2	683.8	0.092	380	579	0.66
		0.4	832.7	0.098	442	644	0.69
		0.6	996.8	0.120	457	661	0.69
Cold Rolling	Longitudinal	0.20	753.1	0.116	367	553	0.66
		0.30	902.0	0.132	402	574	0.70
		0.57	1018.0	0.125	467	673	0.69
AISI 80DF							
Undeformed	Longitudinal	0.0	880.8	0.129	400	406	0.99
	Transverse	0.0	764.1	0.102	406	431	0.94
Balanced Biaxial Stretching	Longitudinal	0.16	969.7	0.107	497	726	0.68
Uniaxial Tension	Longitudinal	0.04	793.9	0.116	387	579	0.67
	Longitudinal	0.05	955.6	0.136	412	624	0.66
	Longitudinal	0.08	979.6	0.136	444	659	0.67
	Transverse	0.08	779.9	0.0916	443	515	0.86

Conversion Factor:
1 ksi = 6.89 MPa

cyclic strength coefficient, K', occurred as a result of the initial prior deformation to an effective strain of 0.2; however, no additional change occurred with further increase in the amount of deformation.

AISI 50XF STEEL - The cyclic and monotonic stress-strain curves for this steel are shown in Figures 12a and 12b and the 0.2CYS and 0.2MYS are shown in Figure 6. As can be seen, the general behavior was the same as in the 1006 steel. The increases in 0.2CYS and 0.2MYS are 21 and 28 MPa (3 and 4 ksi), respectively, per 0.1 increase in effective strain beyond $\varepsilon_{eff} = 0.2$, the same as in 1006.

The 0.2CYS, the 0.2MYS, and the 0.2CYS/0.2MYS ratio are shown in Table 6 and the observations previously made for 1006 apply to 50XF. Comparison of the two steels also shows that, in general, the 0.2CYS/0.2MYS ratio for the 50XF steel is larger than for the 1006 steel (0.68 versus 0.61 on average after deformation),

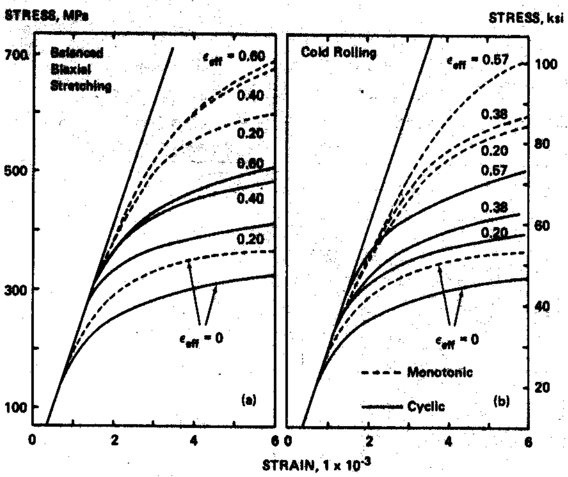

Fig. 12 - AISI 50XF steel–monotonic and cyclic stress-strain curves after deformation

indicating that 50XF cyclically softens slightly less than 1006.

In 50XF, both n′ and K′ decreased with the initial deformation to ε_{eff} = 0.2, as in 1006, Table 6. With further deformation, however, in contrast to 1006, a definite pattern was observed in the variation of K′; K′ increased significantly with increasing prior strain.

AISI 80DF STEEL - The cyclic and monotonic stress-strain curves for this steel are shown in Figures 13a, 13b, and 13c. The 0.2CYS and 0.2MYS values are listed in Table 6 and plotted in Figure 7. The undeformed material is essentially cyclically stable in the longitudinal direction and exhibits minimum cyclic softening in the transverse direction—the 0.2CYS/0.2MYS ratio is 0.99 and 0.94 in these two directions, respectively (Table 6). Both the 0.2CYS and 0.2MYS increased as a result of deformation, Figure 7, but a larger amount of cyclic softening occurred after deformation. The anisotropy observed in the monotonic yield strength after uniaxial tension was completely eliminated by cycling and was not present in the cyclic yield strength. The 0.2CYS/0.2MYS ratio after uniaxial tension is about 0.67 in the direction parallel to the prior tension and 0.86 in the transverse direction (less cyclic softening).

The cyclic stress-strain constants, Table 6, do not appear to vary in a predictable manner as a result of deformation.

SUMMARY AND CONCLUSIONS

The effect of cold forming under different strain states on the strain-controlled fatigue properties of two hot-rolled, vanadium bearing HSLA steel sheets (AISI 80DF and AISI 50XF) was investigated and compared with that of a reference steel, AISI 1006. Three strain states were studied: balanced biaxial stretching (BBS, produced by in-plane stretching), plane strain deformation (produced by cold rolling, CR), and

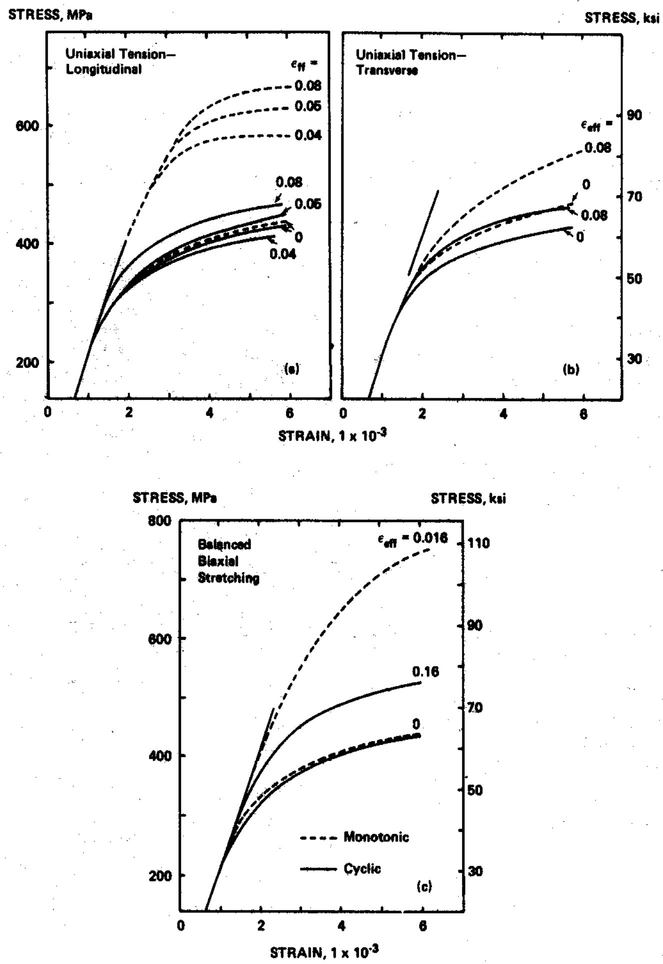

Fig. 13 - AISI 80DF steel–monotonic and cyclic stress-strain curves before and after deformation

uniaxial tension (UT). Effective strain levels ranging from 0.04 to 0.6 were investigated. Cold rolling and uniaxial tension were conducted so that the positive (tensile) principal surface strain was parallel to the hot-rolling direction, HRD. After deformation, the specimens were oriented parallel to the HRD, that is, parallel to the prior tensile surface strain; in addition, after UT they were also oriented transverse to the HRD to assess possible anisotropy effects due to the cold deformation.

The main conclusions are:

- Effect of Prior Deformation on the Total-Strain versus Life Behavior

1) At small strain amplitudes (lives longer than 10^4 to 10^5 reversals), the prior deformation produced an increase in fatigue life, in all three steels.

2) At large strain amplitudes (lives shorter than 10^4 to 10^5 reversals), some differences were observed between the three steels: the fatigue life remained approximately the same, or was decreased by prior deformation in 1006; it was decreased more markedly in 50XF; and it

appeared to remain the same or increased slightly in 80DF.

3) The change in fatigue life (decrease or increase) caused by the prior deformation was generally greater in 50XF than in 1006.

4) The effect of the mode of prior deformation on fatigue life was relatively small. However,

a) Balanced biaxial stretching appeared to be somewhat more detrimental than cold rolling at large cyclic strain amplitudes.

b) Cold rolling produced less scatter in fatigue life at all strain amplitudes than balanced biaxial stretching.

5) No systematic relationship was observed between the level of prior strain and the magnitude of either the decrease or the increase in fatigue life.

- Effect of Prior Deformation on Monotonic and Cyclic Yield Strength

1) The 0.2 percent offset monotonic yield strength, 0.2MYS, increased with increasing prior strain for all modes of deformation. For a given level of prior strain, the 0.2MYS was within the same scatter band for the BBS, CR, and longitudinal UT specimens (specimens parallel to the prior tension). In contrast, the 0.2MYS was much lower for the transverse UT specimens.

2) The 0.2 percent offset cyclic yield strength, 0.2CYS, also increased with increasing prior strain for all deformation modes, although at a slower rate than the 0.2MYS. However, the anisotropy observed after UT in the monotonic yield strength was not present in the cyclic yield strength.

3) In the undeformed condition, cyclic softening occurred in 1006 and 50XF steels while 80DF was essentially cyclically stable. After deformation, cyclic softening occurred in all three steels.

In general, the rather significant effects of the magnitude of the deformation on cyclic strength were not reflected in significant changes in the effect of the amount of deformation on the strain-life properties.

ACKNOWLEDGMENTS

The authors acknowledge the financial support of the American Iron and Steel Institute under contract 1201-409D for a portion of this work. They thank the members of the AISI Task Forces on Structural Research and on Fatigue—Transportation Department, Committee of Sheet Steel Producers—for their interest in this project. Finally, they express their appreciation to Messrs. J. M. Flynn and J. A. Nicholson, U. S. Steel Research Laboratory, for their valuable assistance with the experimental work throughout the course of the project.

REFERENCES

1. Parker, T. E. and G. L. Montgomery, "Effect of Balanced Biaxial Stretching on the Low Cycle Fatigue Behavior of SAE 1008 Hot Rolled Low Carbon Steel," SAE Paper 750048, 1975.

2. Sherman, A. M., "Fatigue Properties of High Strength Low Alloy Steels," Met. Trans., Vol. 6A, 1035-1040, May 1975.

3. Libertiny, G. Z., T. H. Topper, and B. N. Leis, "The Effect of Large Prestrains on Fatigue," Experimental Mechanics, 64-68, February 1977.

4. Pietrowski, R., "The Effect of Forming on the Fatigue Properties of Dofascoloys 50F, 50W, and 50Z," Dominion Foundries and Steel, Ltd., November 3, 1977.

5. Aichbhaumik, D., "Steel Variability Effects on Low Cycle Fatigue Behavior of a Single Grade of High Strength Low Alloy Steel," Met. Trans. A, Vol. 10A, 269-278, March 1979.

6. Holt, J. M., and B. K. Stewart, "Variability of Strain-Controlled Fatigue Properties of USS Dual Phase 80 Steel," SAE Paper 801400, 1980.

7. Barsom, J. M., K. H. Klippstein, and A. K. Shoemaker, "Fatigue Behavior of Sheet Steels for Automotive Applications, A State-of-the-Art Review," Research Report SG 80-2, American Iron and Steel Institute, February 1980.

8. Marciniak, Z., K. Kuczynski, and T. Pokora, "Influence of the Plastic Properties of a Material on the Forming Limit Diagram for Sheet Metal in Tension," International Journal of Mechanical Sciences, Vol. 15, 10, 789-805, October 1973.

9. Holt, J. M., unpublished research.

10. Charpentier, P. L., "The Influence of Deformation Mode During Cold Forming on the Post-Formed Flow and Fracture Behavior of Low Carbon and High Strength Low Alloy Steel Sheets," PhD Thesis, Carnegie-Mellon University, January 1981.

11. Standard Recommended Practice for Constant-Amplitude Low-Cycle Fatigue Testing, ASTM Designation: E606-80, Annual Book of ASTM Standards, Part 10.

12. Peterson, R. E., "Stress Concentration Factors," John Wiley and Sons, 1974.

13. Standard Definition of Terms Relating to Constant-Amplitude, Low-Cycle Fatigue Testing, ASTM Designation: E513-74, (1980), Annual Book of ASTM Standards, Part 10.

14. Raske, D. T. and J. D. Morrow, "Mechanics of Materials in Low Cycle Fatigue Testing," Manual on Low Cycle Fatigue Testing, ASTM STP 465, 1-26.

15. Fatigue Design Handbook, Society of Automotive Engineers, 1968.

16. Sandor, B. I., "Fundamentals of Cyclic Stress and Strain," The University of Wisconsin Press, 41-47, 1972.

17. Proceedings of the SAE Fatigue Conference, P-109, Society of Automotive Engineers, April 1982.

18. Charpentier, P. L. and J. M. Holt, "Effect of Large Prior Monotonic Strains on the Fatigue Behavior of Hot-Rolled AISI 1006 and AISI 50XF steels," American Iron and Steel Institute, Research Report, in preparation.

19. Holt, J. M., "Strain-Controlled Fatigue Properties of Hot-Rolled DQSK Steel Compared with Those of EX-TEN F50 and Dual Phase 80 Steels," SAE Paper 810434, Society of Automotive Engineers, February 23-27, 1981.